Chemical Engineering Journal 293 (2016) 55–67

Contents lists available at ScienceDirect

Chemical Engineering Journal

journal homepage: www.elsevier.com/locate/cej

Effects of particle size on CO_2 reduction and discharge characteristics in a packed bed plasma reactor

T. Butterworth *, R. Elder, R. Allen

Department of Chemical and Biological Engineering, University of Sheffield, UK

HIGHLIGHTS

- Packing particle size is a dominant parameter in packed bed plasma reactors.
- Larger particle sizes typically lead to lower conversion.
- Smaller particle sizes increase breakdown voltage and leads to partial discharging.
- Partial discharging causes significant decreases in reactor performance.
- Methodology for quantification of partial discharging is demonstrated.

GRAPHICAL ABSTRACT

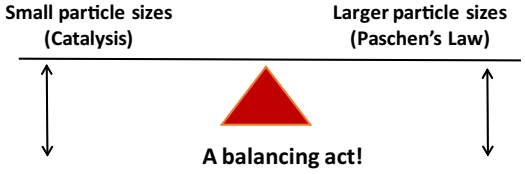

ARTICLE INFO

Article history:
Received 28 December 2015
Received in revised form 12 February 2016
Accepted 13 February 2016
Available online 17 February 2016

Keywords:
Plasma
Packed bed reactor
Plasma catalysis
Particle size
CO2 reduction
Dielectric barrier discharge

ABSTRACT

Current understanding of the behaviour of plasma discharges within packed bed reactors (PBRs) is very poor, and the effects of many of the parameters that can be varied are still unknown. This article investigates the effects of particle size (180 μm–2000 μm) of two different commonly used packing materials (Al_2O_3 and $BaTiO_3$) on the conversion of CO_2 in PBRs. The reactor behaviour is observed through determination of product gas composition and plasma power consumption in order to determine CO_2 conversion and reactor efficiency. Electrical characterisation techniques are used to determine reactor burning voltage, and capacitances. These capacitances are subsequently used to quantify the occurrence of reactor partial discharging over a range of different operating conditions.

The results indicate that smaller particles (down to 180 μm) can significantly increase CO_2 conversion by up to 70%, provided that the voltage applied is sufficiently high to generate a discharge in the void spaces of the packing material. However, with decreasing particle size, the reactor burning voltage is found to increase rapidly, as well as the tendency of the reactor towards partial discharging.

1. Introduction

Packed bed dielectric barrier discharge (DBD) reactors are one of the most widely investigated plasma-based technologies for industrial gas processing, yet their behaviour is poorly understood. Packing particle size effects discharge phenomena and chemistry within the packed bed, and can therefore impact conversion and efficiency of a process. Reduction of CO_2 to CO in non-thermal plasma is a particularly challenging reaction as it tends to be limited in either conversion or efficiency. The introduction of catalytic materials into the plasma discharge can lead to a synergistic effect [1], which may allow the efficient conversion of CO_2 – consequently overcoming the limitations currently encountered in other CO_2 plasma reduction techniques.

PBRs can have a wide range of different packing materials, with commonly used examples being ferroelectrics such as $BaTiO_3$, ceramics such as Al_2O_3, or materials more commonly found in thermally activated catalytic systems, such as ceramic supported transition metal catalysts. PBRs have a wide range of possible

* Corresponding author.
E-mail address: t.butterworth@sheffield.ac.uk (T. Butterworth).

http://dx.doi.org/10.1016/j.cej.2016.02.047
1385-8947/

applications, having been investigated for the reduction of CO_2, destruction of organic pollutants [2], reduction of NOx [3], and reforming of CH_4 [4]. Diagnostics of PBRs is very challenging as they are highly complex systems with many parameters that can influence their behaviour, yet the optical techniques that are commonly used in other plasma systems are either very difficult or impossible. Modelling [5,6] and experimental work [7] is helping to progress understanding of discharge phenomena within the reactors, but a lot of progress is still to be made.

Non-thermal plasma systems are characterised by high populations of chemically reactive species, such as radicals, ions and excited states that are able to participate in reactions that would not occur in a more conventional chemical reactor. In plasma catalysis it is believed that the catalyst packed reactor becomes activated in some way by the presence of the plasma, this can occur by inducing the formation of reactive species in the gaseous phase [8], or activation of the catalyst itself [9].

The reactive species found in plasma can have a wide range of lifetimes, with time frames ranging from picoseconds to minutes. Consequently, species lifetime and mobility (a function of species mass, charge and local electric field strength) dictate the length that a species can travel before it participates in a reaction. Direct interaction between a catalyst and a reactive species is dependent upon the distance between the plasma discharge and the catalyst surface, as well as the species migration and diffusion lengths. Highly mobile species, such as electrons, or metastable species, such as OH, can have diffusion lengths of ~60 μm, whilst heavy, short lifetime species such as $O(^1D)$ may travel <1 μm [7].

Therefore, if the plasma-catalytic effects are due to specific excited species it is essential that these species are able to interact with catalyst surfaces before relaxation or quenching occurs. One of the paradigms of heterogeneous catalysis is the requirement for a high surface area to volume ratio. This paradigm becomes even more important in plasma catalytic systems due to the very short species lifetimes, meaning that the surface area of the catalyst-plasma interface should be maximized. Consequently, this implies that small, tightly packed catalyst particles would be optimal for a plasma-catalytic system. However, small particles will create small interparticulate void spaces that are likely to inhibit the formation of plasma if an insufficient electric field strength is applied. This prediction is based on Paschen's law, which relates the minimum breakdown voltage of a gas to the electrode spacing and system pressure [10].

Therefore, there is a balance to be achieved between the high surface area to volume ratio required for optimum performance of a catalyst, and the constraints on minimum particle size that can be predicted by Paschen's law. Additionally, conversion and efficiency of PBRs can be effected by a wide range of experimental parameters, including gas composition, residence time, electrical properties (frequency, voltage, polarity), and packing material properties (dielectric constant, porosity, etc.)

There are two research questions that are tested in this article:

- What effect does particle size have on the performance of a PBR for CO_2 reduction?
- Why does particle size cause these changes in reactor performance?

2. Experimental method

The experimental work is split into two sets of experiments. The first experiment treats the reactor as a "black box", i.e. a range of experimental parameters are tested and the resultant effect on reactor outlet gas composition and power consumption is monitored. Three different gas compositions are tested, pure CO_2, 50% Ar–50% CO_2, and 90% Ar–10% CO_2. The addition of argon to CO_2 is used to reduce the breakdown voltage of the gas mixture. The reactor is driven by a 5 kHz square wave, with applied voltage amplitudes ranging from 5 to 10 kV.

The second experiment seeks to understand the behaviour of the reactor that is observed in the first experiment through monitoring of 3 electrical signals: applied voltage, instantaneous current and charge transferred in the reactor. A partial discharging equivalent electronic circuit is applied so that important operational parameters such as the burning voltage, and reactor capacitances can be obtained. These reactor capacitances are in used to quantify the extent of partial reactor discharging, and consequently to explain the trends observed in the first set of experiments. A range of different gas mixtures, operating frequencies, applied voltages and wave shapes are applied as required.

2.1. Experimental set-up

The experiment is carried out using 2 different packing materials, Al_2O_3 (Sigma-Aldrich) and $BaTiO_3$ (Catal International Ltd) with 5 different particle sizes: 180–300 μm, 300–500 μm, 500–850 μm, 850–1400 μm, and 1400–2000 μm. Surface area of the 3 mm pellets, determined by BET analysis, is ~358 m^2/g for Al_2O_3 and is less than 0.1 m^2/g for $BaTiO_3$. Dielectric constant of the $BaTiO_3$ is experimentally determined to be $\varepsilon = 4000$ at 25 °C and 1000 Hz. Under the same conditions the dielectric constant of the Al_2O_3 is assumed to be 10. The particles are random in shape, and are produced by crushing 3 mm pellets and subsequently sieving the remains using stainless steel test sieves (Retsch) and a vibratory sieve shaker (Retsch AS 200 Control) to achieve the desired size distributions.

The reactor body is a co-axial geometry fabricated from quartz glass with a 15 mm outer diameter, with a 1 mm wall thickness. The live electrode is a stainless steel rod with a diameter of 3 mm, positioned in the centre of the glass tube. The ground electrode is a silver paint that is applied to the outside of the quartz glass tube, having a length of 18 mm. The packed bed extends an additional 5 mm either side of the electrode. This gives an inter-electrode spacing of 6 mm, and an active plasma volume of ~2.3 cm^3 with a bed volume of ~3.5 cm^3.

The power source is a high voltage power amplifier (Trek 10/40A-HS) with a maximum output (peak) voltage of 10 kV. The input signal to the high voltage amplifier is generated via Labview by a National Instruments DAQ USB-6211. Voltage is monitored using a differential high voltage probe (Tektronix P6015A), current pulses are observed using a wide band current transformer (Pearson Electronics 6595). Plasma power is determined in real time with Labview by using the so-called "capacitor method" (described in Section 2.2), using a 250 V, 47 nF polyester layer capacitor, with the potential difference over the capacitor monitored using an 10:1 oscilloscope probe (Picoscope TA133). All of the electronic sampling equipment is connected to a USB oscilloscope (Picoscope 6404C) with a sample interval time of 800 ps. Feed gas flow rate is fixed at 100 ml/min total flow rate, with the gas composition being CO_2 balanced with argon. Three different gas compositions are tested in the first experiment: pure CO_2, 50% CO_2 and 10% CO_2. The outlet gas composition is determined by mass spectrometry (MS) (Hiden QGA) and Fourier Transform Infrared Spectroscopy (FTIR) (Varian 660IR).

An overall schematic of the experimental set-up is shown in Fig. 1.

2.2. Determination of product gas composition

Measurement of CO_2 conversion is calculated with data obtained from the mass spectrometer. Continuous monitoring of the mass-to-charge (m/z) ratios at $m/z = 28$, 32, 40 and 44 is used to elucidate the product gas composition. The independent and

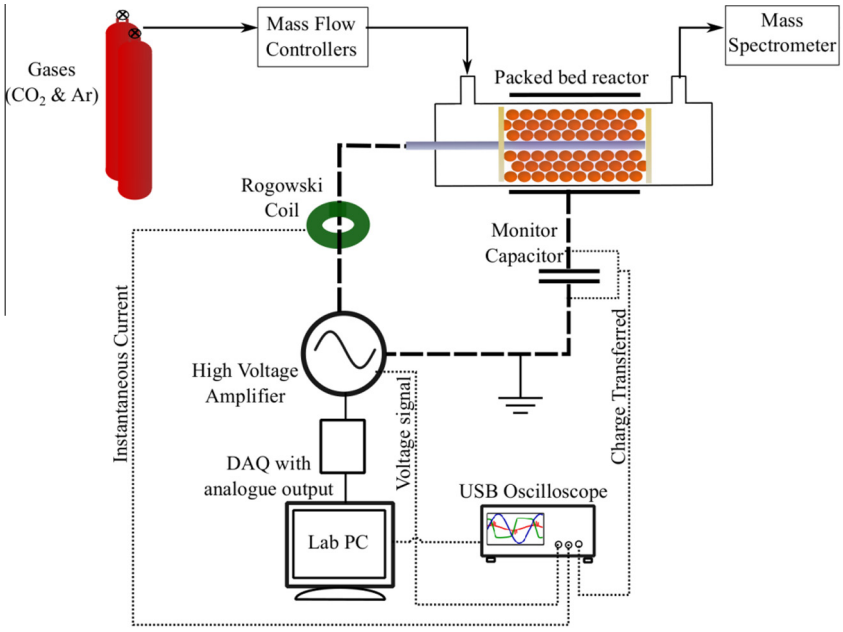

Fig. 1. Experimental schematic.

characteristic signal for CO_2 occurs at $m/z = 44$, and therefore it is used for measuring CO_2 concentration. Argon is used as an internal standard in the mass spectrometer in order to account for fluctuations in instrument pressure, reactor outlet gas volumetric flowrate and gas temperature.

CO_2 conversion is calculated using Eq. (1):

$$CO_2 \text{ Conversion } (\%) = \frac{[CO_{2\,in}] - [CO_{2\,out}]}{[CO_{2\,in}]} \times 100 \quad (1)$$

Data from the MS and FTIR show that CO and O_2 are the major gaseous reaction products having a ratio of 2:1, with a combined yield approaching one. The only gaseous byproduct observed is ozone, this is determined using the FTIR based on the characteristic peak at 1055 cm^{-1}, however the concentration does not exceed 800 ppm, and values are typically less than than 150 ppm at steady state. No evidence for the formation of solid or liquid reaction products is observed.

2.3. Evaluation of electrical parameters

Some of the physical properties of DBDs and PBRs can be obtained by analysis of their electrical characterisics. Typically, 3 different reactor electrical signals are monitored, the applied voltage to the reactor ($V(t)$), the instantaneous current ($i(t)$), and the charge transferred ($Q(t)$) in the reactor.

Shown in Fig. 2 is a diagram showing the typical appearance of the signals obtained from a sine wave driven DBD reactor with a monitor capacitor connected in series after the reactor. The blue line shows the reactor applied voltage, and from it the voltage amplitude and frequency can be obtained. The red line shows the instantaneous current in the reactor, which is composed of a displacement current (approximately a sine wave) with a number of microdischarges (superimposed pulses). The microdischarges are characterised by fast, dynamic pulses having very short rise times (<10 ns) with individual microdischage pulse durations ranging from 10–150 ns. The reactor charge transferred is measured using a "monitor capacitor" situated in series with the DBD between the reactor and the ground. The potential difference ($V_m(t)$) measured across the capacitor is multiplied by its capacitance (C_m, assumed to be constant with change in frequency) to obtain the instantaneous charge on the capacitor ($Q_m(t)$). This instantaneous charge on the monitor capacitor is shown by the green signal in Fig. 2. As the monitor capacitor is in series with the DBD, the current through both the reactor and the capacitor must be equal. The measured charge on the capacitor is therefore equal to the charge transferred through the reactor (see Fig. 3).

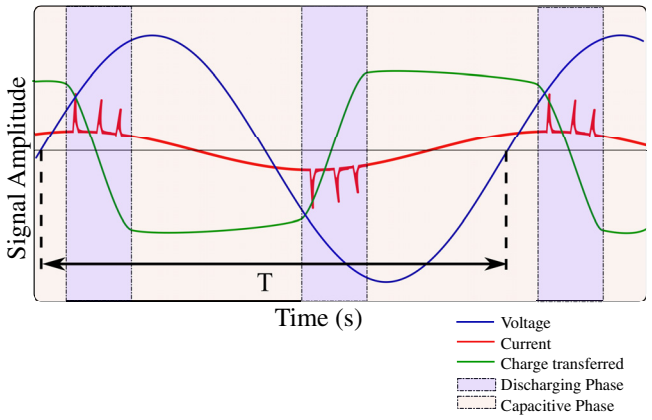

Fig. 2. Typical appearance of signals obtained from a sinusoidally driven DBD reactor operating in the filamentary mode. A DBD goes through sequential discharging and capacitive phases that are can be related to an equivalent electrical circuit in order to obtain important operational characteristics.

A plot of $Q_m(t)$ versus $V_m(t)$ generates a hysteresis loop known as a Lissajous figure. It can be shown that the area contained by the Lissajous figure is equal to the energy discharged in the reactor in one complete DBD discharge cycle (T). Multiplying this value by the frequency of the applied voltage signal gives an accurate measurement of the plasma power [11]. The 4 sides of the Lissajous figure correspond to the 4 phases that occur during the DBD discharge cycle. There are two "discharging phases" and two "capacitive phases", which occur with the successive positive and negative phases of the applied AC voltage [12]. The relationship between these different phases and the transient discharge occurring within the DBD is well documented [13].

In addition to the plasma power, the Lissajous plot can also be used to obtain other important reactor characteristics, such as

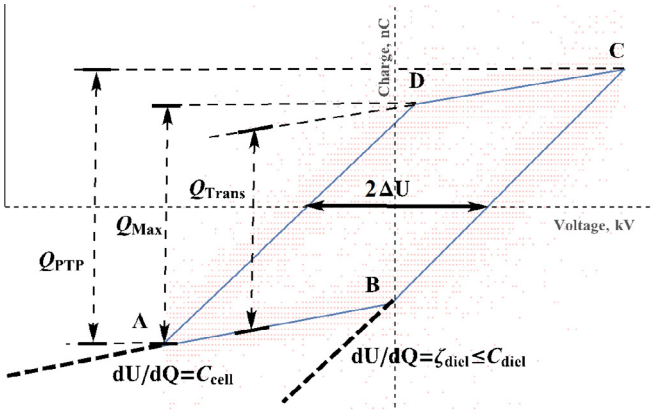

Fig. 3. Annotated Lissajous figure, showing the fitted linear models and the raw data that it is applied to. The annotation shows the data that may be obtained from the plot.

the burning voltage (U_b, calculated from ΔU), reactor charge (Q_{max}, Q_{PTP}, & Q_{trans}), and reactor capacitances (C_{Cell}, C_{diel} and ζ_{diel}). The reactor capacitances, C_{cell} and C_{diel}, correspond with physical properties of the reactors and can be related to a DBD by an equivalent electrical circuit. The simplest representation of a DBD equivalent electrical circuit for a DBD is shown in Fig. 4.

Relating the equivalent electrical circuit to the Lissajous figure. The lines AB and CD correspond to the "discharge off" or capacitive phase. During this time, no plasma is present in the reactor and consequently no charge is transferred between the electrodes. The gradient of the lines AB and CD is therefore equal to C_{cell} during this phase. Where C_{cell} is composed from the gap capacitance (C_{gap}) and the dielectric capacitance (C_{diel}), applying Kirchoff's laws this is shown by equation:

$$\frac{1}{C_{cell}} = \frac{1}{C_{diel}} + \frac{1}{C_{gap}} \tag{2}$$

Lines *BC* and *DA* are the "discharging phase" of the discharge, i.e. when a plasma breakdown occurs. The gradient of these lines should, theoretically, be equal to the capacitance of the dielectric (C_{diel}) for a "fully bridged gap". As current begins to flow through the reactor, the gap ceases to act as a capacitor and the term C_{gap} is negated. C_{diel} is fixed for a particular reactor and is determined entirely by the choice of dielectric material and the geometry of the DBD. If the gap is not "fully bridged", i.e. not all of the charge accumulated on the dielectric layer is transferred during the plasma discharge phase, the value of the capacitance measured from the gradient of the lines *BC* and *DA* is less than value of C_{diel}, and is termed the effective dielectric capacitance, ζ_{diel}. In the case of a non "fully bridged gap" the reactor can be described as partially discharging. Partial discharging occurs due to some areas of the electrode not becoming saturated with microdischarges [14,15]. Saturation of the electrodes, and consequent full charge bridging of the gap tends to happen through the application of voltages that greatly exceed the breakdown voltage [15] or reportedly through the usage of packing materials [16].

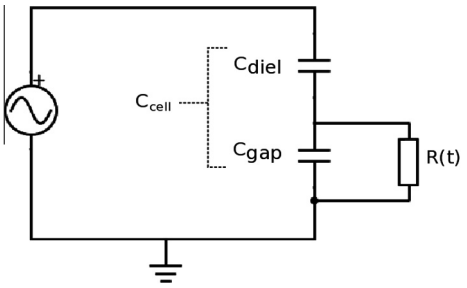

Fig. 4. Simplest equivalent circuit of a DBD.

For a partially discharging DBD the alternative equivalent electrical circuit model of Peeters and van de Sanden (Fig. 5) is required to accurately reflect the reactor behavior. This alternative equivalent geometry splits the circuit into a non-discharging (α) fraction, and a discharging fraction (β).

This alternative equivalent electrical circuit and accompanying mathematical treatment, addresses the problem of the calculated (a.k.a. effective) dielectric capacitance from the Lissajous figure (ζ_{diel}), being less than the value of C_{diel}. In instances where partial reactor discharging is occurring, mathematically treating the Lissajous figure as the simplest equivalent circuit shown in Fig. 4 can give artificially low values for the reactor burning voltage and charge transfer. The corrected equation, derived in [14], to calculate burning voltage is given by Eq. (3):

$$U_b = \frac{1 - C_{cell}/C_{diel}}{1 - C_{cell}/\zeta_{diel}} \Delta U \tag{3}$$

In a packed bed reactor, the capacitance of the packing material should also be taken into account. Mei et al. [16] have proposed a simple model where the gap capacitance, C_{gap}, is treated as the capacitance of the gas (C_{gas}) and packing material ($C_{packing}$) as though they were two parallel plate capacitors in series. Although this is a simplified relationship, it is a reasonable approximation for practical application. The actual capacitive behavior of the packed bed is more complex than this model, however it cannot be easily described by a simple mathematical relationship. In reality, each packing particle would act as an individual capacitor of unknown capacitance. However, this approach to equivalent circuit modeling would be very difficult to apply in reality.

The model used in this article is that of Peeters and van de Sanden, as the focus of the work is on the change of the plasma discharge behavior and burning voltage with different particle sizes.

3. Results and inference

3.1. Gas conversion results and inference

Shown in Fig. 6 is CO_2 conversion plotted against plasma input power in an Al_2O_3 (Fig. 6a–c) or $BaTiO_3$ (Fig. 6d–f) packed bed at CO_2 inlet concentrations of 10% (Fig. 6a and d), 50% (Fig. 6b and e), and 100% CO_2 (Fig. 6c and f), with the balance made up with argon. It is important to note when comparing these figures that the total gas flowrate is maintained at 100 ml/min. This is to keep gas residence time in the reactor constant for the empty reactor. This has a significant impact on the percentage conversion

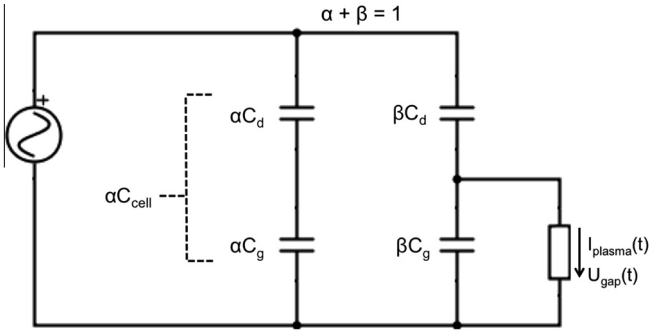

Fig. 5. Alternative equivalent circuit of a partially discharging DBD, presented by Peeters and van de Sanden [14].

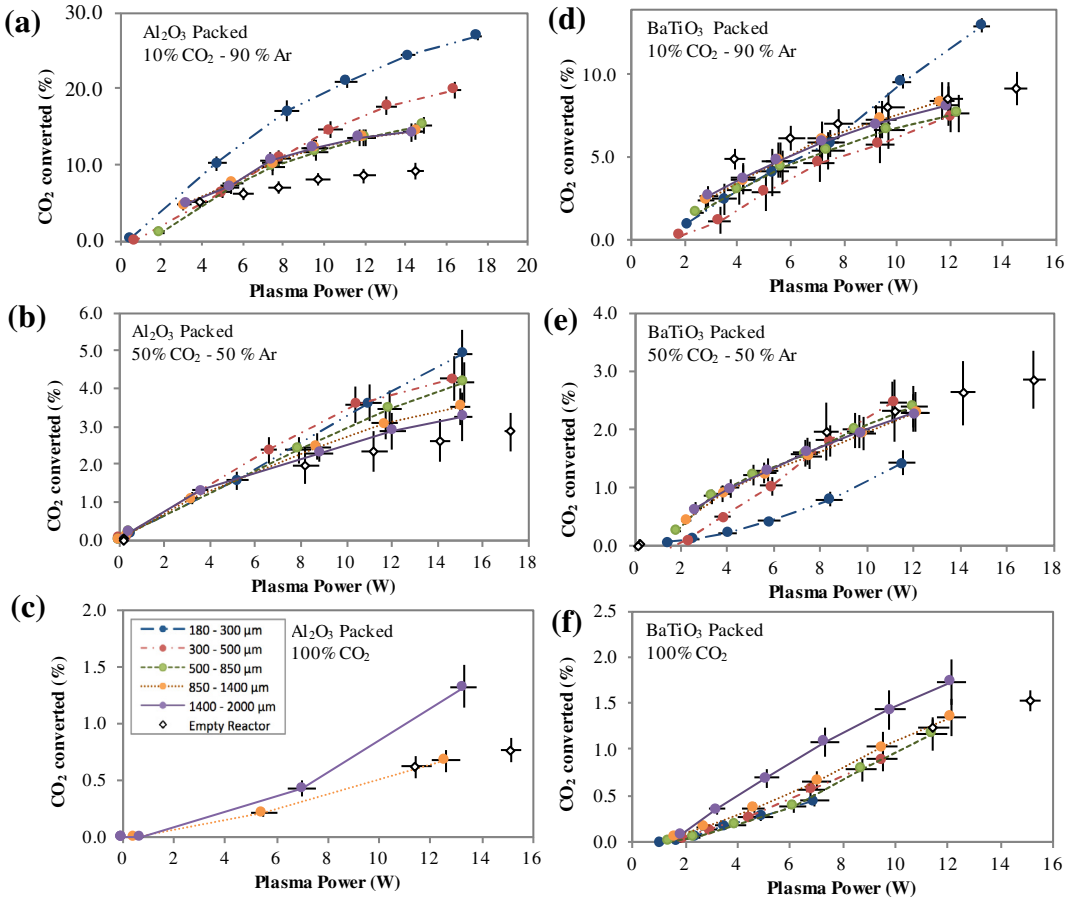

Fig. 6. CO_2 conversion plotted against plasma power in Al_2O_3 (a–c) and $BaTiO_3$ (d–f) packed beds. 3 different gas compositions are used: 90% Ar–10% CO_2 (a and d), 50% Ar–50% CO_2 (b and e), and 100% CO_2 (c and f). Total gas flow rate is maintained at 100 ml/min. Reactor is driven by a 5 kHz square wave, with applied voltage amplitude stepped between 5 and 10 kV. Error bars indicate one standard deviation.

when higher concentrations of CO_2 are used. In order to attempt to compensate for this the data may also be compared on the basis of absolute CO_2 conversion, as shown in Fig. 7. Additionally, it should be noted when comparing PBRs with the empty reactor that the presence of packing material decreases the gas residence time by up to ~70% with the smallest particles, which is expected to have a negative effect on CO_2 conversion.

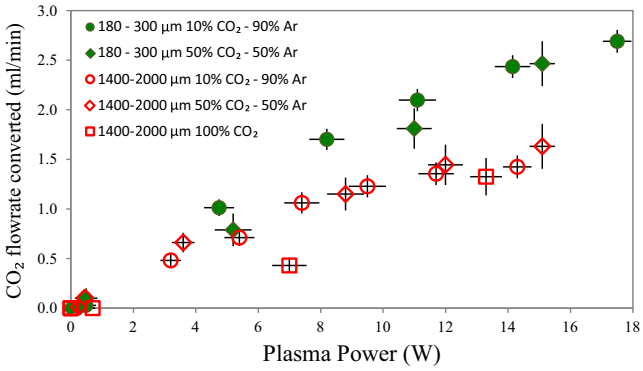

Fig. 7. CO_2 flow converted plotted as a function of plasma power in an Al_2O_3 packed bed with particle sizes of 180–300 µm (green filled plot markers) and 1400–2000 µm (red hollow plot markers). N.B. 100% CO_2 data is not included for the 180–300 µm particles, as no plasma is formed in the packed bed. (For interpretation of the references to colour in this figure legend, the reader is referred to the web version of this article.)

Fig. 6 shows a number of trends, each of which is addressed with a further explanation in the following paragraphs:

(a) Particle size has a large effect on CO_2 conversion.
(b) Changing particle sizes causes a change in the behavior of the plasma discharge.
(c) Al_2O_3 can increase CO_2 conversion compared with both a $BaTiO_3$ packed and an empty reactor.
(d) $BaTiO_3$ reduces the reactor breakdown voltage compared with an Al_2O_3 packed and an empty reactor.

3.1.1. Evidence for trend a. – Particle size has a large effect on CO_2 conversion

The data presented in Fig. 6 shows that in almost all cases, particle size has an effect on CO_2 conversion. In some cases the smallest particle sizes lead to a very large increase in conversion. The most clear example of this is observed with the 90% Ar–10% CO_2 gas mix in the Al_2O_3 packed bed. Fig. 6a shows with 180–300 µm, and 300–500 µm particles that conversion can be up to 26.9% and 19.9% respectively. At ~14 W plasma power CO_2 conversion with the 180–300 µm bed is 24.3%, with 300–500 µm it is 18.3%, and with larger particle sizes conversion ranges from 14.3% to 15.1%. This is an increase of up to 70% and 28% respectively for the same applied power. Comparing this with Fig. 6d – the $BaTiO_3$ packed bed at 90% Ar–10% CO_2, it can be seen that only the 180–300 µm particles lead to a significant increase in CO_2 conversion compared to other particle sizes, and only at powers greater than 10 W. With the next smallest particle size, 300–

500 μm, the CO_2 conversion at any plasma power is the lowest of the group.

As CO_2 concentration is increased, the benefits of using small particle sizes tends to reduce. Fig. 6b. shows the 50% CO_2–50% Ar mix in Al_2O_3 packed beds. Interestingly, at the highest input powers tested the CO_2 conversion decreases sequentially with increasing particle size. The difference in conversion between the smallest and largest particles at a power of ~15 W is now reduced to ~54% (compared with ~70% at 14 W in 90% Ar–10% CO_2). In the $BaTiO_3$ packed bed with the 50% Ar–50% CO_2 mix (Fig. 6e), CO_2 conversion is lowest with the 180–300 μm particles, followed by the 300–500 μm particle sizes, with the large particle sizes having very similar conversions to each other for any input plasma power.

With the 100% CO_2 experiments the benefits of small particle sizes are completely negated. No CO_2 conversion is found to occur in the Al_2O_3 packed bed with particle sizes less than 850 μm. Similarly, in both the empty reactor and the Al_2O_3 packed reactor, no CO_2 conversion is observed at voltages less than 8 kV – this is due to no plasma forming in the reactor at these conditions. With the $BaTiO_3$ packed bed, CO_2 conversion is observed with every particle size at applied voltages down to 6 kV. In both the $BaTiO_3$ packed bed, and the Al_2O_3 packed bed the highest CO_2 conversion occurs with the largest particle sizes, and CO_2 conversion decreases sequentially with particle size.

To conclude, small particle sizes can lead to either an increase or decrease in CO_2 conversion. This appears to be dependent upon the concentration of argon used in the feed gas mix. Higher argon concentrations lead to an improved conversion of CO_2 in smaller particle sizes, where as low argon concentrations are preferential for CO_2 conversion in larger particle sizes. The effects of gas composition on CO_2 conversion therefore requires further analysis in order to understand the effect it has, and ultimately to understand the influence of particle size.

3.1.2. Effect of changing gas composition

In this experiment argon is used to reduce the breakdown voltage of the gas mixture in order to study the effect of particle size. However, by changing the gas composition, other effects are also observed. Fig. 6 suggests that by changing the gas composition from low to high concentrations of CO_2 reduces CO_2 conversion. There are two likely causes for this trend:

Noble gasses create alternate reaction pathways [17,18] and increase electron and ion densities [17] that will promote CO_2 conversion. They may also induce enhanced reactivity of the packing materials.

Total gas flow rate is kept constant at 100 ml/min. Therefore with increased CO_2 concentration, the volumetric flowrate of CO_2 increases, and the specific energy input per molecule of CO_2 decreases.

Consequently, this lower specific energy input, combined with the changes in plasma chemistry associated with noble gasses, reduces the percentage CO_2 conversion at high CO_2 concentrations. Reactor performance can also be evaluated on the basis of flowrate of CO_2 converted, which simplifies comparison between packing materials when different gas compositions are tested.

Fig. 7 shows the effect of different gas compositions on the flowrate of CO_2 converted for two different particle sizes of Al_2O_3, 180–300 and 1400–2000 μm. Plotting the different gas compositions together allows the benefits of small particle sizes to be easily observed. As plasma power increases it can be seen that the CO_2 conversion tends towards a plateau. At high plasma powers (>14 W) this conversion plateau is approximately ~70% higher in the small particle sizes compared with the large ones. This is strong evidence for the benefits of small particle sizes of Al_2O_3 for CO_2 conversion in PBRs, provided that a discharge can be ignited in the packed bed.

There is an outlying point for 1400–2000 μm Al_2O_3 at 100% CO_2. This may be attributed to an inability to form discharges in large fractions of the packed bed with this reactor operating condition. This inability to form plasma discharges is the phenomenon termed "partial discharging", the conditions under which this occurs and a method to quantify it are shown in Section 3.2. Higher argon concentration in the gas mix facilitates the formation of plasma at a lower applied voltage. This does not necessarily indicate that high argon concentrations are required to ignite plasmas in small particle sizes, but rather that larger electric fields strengths are required when CO_2 concentration is high.

3.1.3. Evidence for trend b. – Changing particle size causes a change in behaviour of the plasma discharge

Insufficient electric field strength can limit formation of individual discharges in small particle size packed beds. In a PBR, the plasma and the packing material have an interdependent relationship. Therefore, change in particle size is also likely to have an effect on the nature of the plasma in the packed bed, effecting plasma formation and propagation.

In each of these experiments the applied voltage to the reactor is fixed and the power of the plasma in the reactor is measured. Fig. 6 shows that at each applied voltage there is a change in the power of the plasma in the reactor between different particle sizes. For example, looking at Fig. 6a, for each particle size there are differences in the plasma power at the highest powers, despite all being measured using an applied potential difference of 10 kV. This trend can be visualised more easily by comparing the applied voltage to the reactor with the plasma power deviation from the mean, as shown in Fig. 8 for the Al_2O_3 packed reactor with 90% Ar–10% CO_2. The graph shows quite significant differences in plasma power between particle sizes at different applied potential differences. At an input voltage of 10 kV, the power drawn by the reactor with the 180–300 μm and 300–500 μm particles exceeds the power drawn at large particle sizes by up to 3 W. At lower applied voltages, the smaller particles draw less power than the larger particles, with the empty reactor drawing the most power. These differences in power between particle sizes at equal applied voltages are indicative of a change in the behavior of the plasma in the reactor, and they can be seen to be occurring to some extent in every experiment.

At low input voltages or with high CO_2 concentrations it can be shown that the decrease in plasma power with smaller particles sizes is likely to be due to partial discharging in the reactor, further

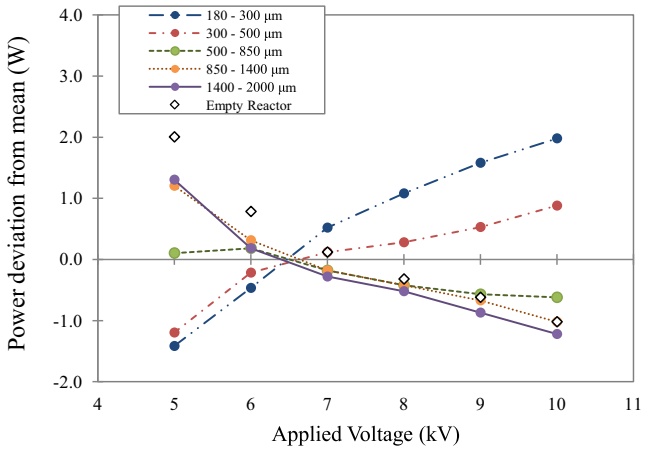

Fig. 8. Measured plasma power deviation from the mean versus applied reactor voltage for an Al_2O_3 packed bed with 90% Ar–10% CO_2 gas mix. Percentage error in measured power does not exceed 6%. "Mean power" is the mean power of each the different particle sizes at any given applied voltage.

evidence for this is presented in Section 3.2. At high applied potential differences or high argon concentrations, the increase in power drawn by the smallest particle sizes is more difficult to explain, although evidence presented in Section 3.3 indicates that the behavior of the plasma changes with very small particle sizes.

3.1.4. Evidence for trend c. – Al_2O_3 can significantly increase CO_2 conversion compared with both a $BaTiO_3$ packed and an empty reactor

The CO_2 conversion in the Al_2O_3 packed bed with all particle sizes and gas compositions always exceeds the conversion in both the empty reactor and the $BaTiO_3$ packed reactor for any plasma power tested (Fig. 6). Additionally, the CO_2 conversion in the empty reactor exceeds that in the $BaTiO_3$ packed reactor in the cases where the feed gas composition is 10% or 50% CO_2, shown in Fig. 6c and d. (With a notable exception – 180–300 μm $BaTiO_3$ particles in 10% CO_2 at high powers.)

There is an exception to trend *c* – in the $BaTiO_3$ packed reactor using 100% CO_2 with 1400–2000 μm particles, at the highest powers tested, the CO_2 conversion exceeds that obtained in the Al_2O_3 packed and empty reactor cases. This is likely to be caused by either partial discharging or poor gas–plasma contacting occurring in the Al_2O_3 packed bed and empty reactor.

The reason for the higher CO_2 conversion in Al_2O_3 compared with $BaTiO_3$ is not clear; there may be a number of possible causes. However, if the reactor were only operated in pure CO_2, it might appear as though $BaTiO_3$ were the superior packing material, even though this is clearly not the case. It must therefore be stressed that care must be taken to ensure optimal discharging of the reactor when making comparisons between materials.

3.1.5. Evidence for trend d. – $BaTiO_3$ greatly reduces the reactor breakdown voltage compared with an Al_2O_3 packed or empty reactor

One of the main benefits that is often attributed to the use of packing materials in a PBR is a reduction in the breakdown voltage of the reactor.

Fig. 6c and f show that CO_2 conversion in a $BaTiO_3$ packed reactor occurs in smaller particle sizes and at lower voltages than with both the empty and Al_2O_3 packed reactors. As stated previously, CO_2 conversion in the empty and Al_2O_3 packed reactor does not occur at in pure CO_2 streams at applied voltages lower than 8 kV, where as with the $BaTiO_3$ packed reactor conversion occurs down to 5 or 6 kV. This is due to plasma being unable to form in the cases where no conversion is occurring. This effect can only be attributed to $BaTIO_3$ reducing the breakdown voltage of the reactor, this is likely to be caused by the very high dielectric constant of the material causing significant enhancement of local electric field strengths.

3.2. Reactor electrical characterization results and inference

Electrical characterization is used in order to provide further evidence, and to explain, the 4 observed trends that are made based on the data presented in Fig. 6.

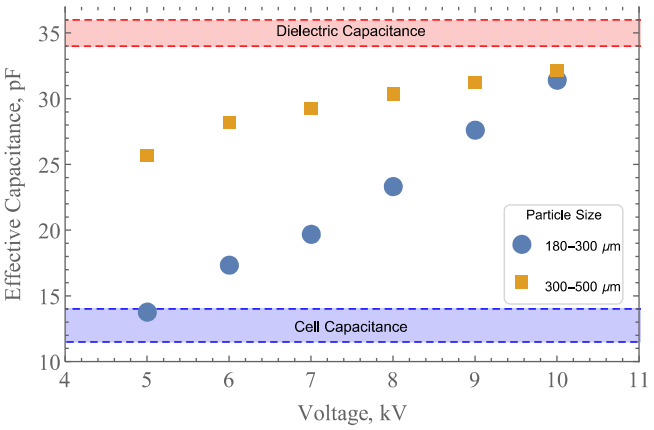

Fig. 9. Measured mean effective capacitance of a 180–300 μm $BaTiO_3$ packed reactor in 90% Ar–10% CO_2 at a range of applied voltages.

3.2.1. Determination of C_{diel} and C_{cell}

The reactor dielectric capacitance, C_{diel}, is measured as 35 pF ± 1 pF. This measurement is made by operating the reactor with a 5 kHz sine wave at 10 kV, using a feed gas composition ranging from 90% to 100% Argon balanced with CO_2. The value for C_{diel} is determined from the mean gradient of the lines BC and DA from the Lissajous figure. There is a slight discrepancy in the measured values of C_{diel} obtained for the positive and negative discharging phases, but this can be explained by the asymmetry of the reactor. Although this value of C_{diel} only provides an estimate for dielectric capacitance, it is difficult to determine a more accurate measurement, therefore this is the value used for the dielectric capacitance of the reactor henceforth. Its suitability as a value for C_{diel} is reflected in the observed saturation of reactor capacitances with other packing materials that is presented in later results.

A value for C_{cell} for each reactor set-up must also be known. However, as stated previously C_{cell} is dependent upon C_{gas} and $C_{packing}$, which in turn are dependent upon gas composition, material dielectric constant, size, shape, and packing density, all of which are variables in this experiment. It is found that the greatest change in the measured value of C_{cell} is with either a change in the reactor packing material, or when pure argon is used in the reactor. Particle size only has a quantifiable effect on the value of C_{Cell} in the $BaTiO_3$ packed reactor. The range of cell capacitances identified is shown in Table 1.

3.2.2. Partial discharging examples

With the values of C_{cell} and C_{diel} defined, cases where $\zeta_{diel} < C_{diel}$ can be examined. Fig. 9 shows some example data for the voltage dependence of ζ_{diel} with 180–300 μm and 300–500 μm $BaTiO_3$ particles.

Fig. 9 shows that with the 180–300 μm particles that the measured value for effective capacitance decreases with decreasing applied voltage almost linearly, from the point at 10 kV, where ζ_{diel} is at ~32 pF, approximately ~3 pF less than C_{diel}, to the point at 5 kV where ζ_{diel} is almost equal to C_{cell}. This indicates a transition from almost full discharging of the reactor, with complete charge

Table 1
Cell capacitances for the reactors with different packing materials, gas compositions and particle sizes.

Reactor condition		Cell capacitance range – pF (0–100% Argon)				
Non-packed reactor		3.2–13				
Al_2O_3		4–14				
$BaTiO_3$	Size (μm)	180–300	300–500	500–850	850–1400	1400–2000
	C_{cell}	11.5–14	12.5–15	12.8–17	13–17.5	13.8–18

transfer from one electrode to the other, to almost no discharge occurring. For comparison, the 300–500 μm $BaTiO_3$ particles show ζ_{diel} decreasing with applied voltage, however in this case the minimum value is ~25.3 pF at 5 kV, indicating that a significant proportion of charge is transferred from one electrode to the other. This figure shows an example where reducing the applied electric field in the reactor causes increased partial discharging with decreasing particle sizes.

At low applied voltages it becomes increasingly challenging to accurately fit linear models to the Lissajous data due to a poor signal to noise ratio. Consequently, in order to increase the accuracy of the linear regression methods used, many of the experiments use an applied voltage of 10 kV whilst changing inlet gas composition. This still allows the effects of particle size on discharge characteristics to be observed, whilst increasing the accuracy of the obtained data.

3.2.3. Measured and corrected burning voltage

The purpose of measuring the effective dielectric capacitance is to quantify the incidence of partial discharging and to correct the calculated values of reactor burning voltage. Theoretically, burning voltage for any individual void space in which a discharge can occur should be constant, regardless of applied voltage. Once the applied voltage reaches a threshold voltage, an electrical breakdown will begin to occur in the individual void. Peeters and van de Sanden [14] demonstrated that the burning voltage is almost constant as a function of applied voltage amplitude in a fixed geometry DBD plasma jet. Shown in Fig. 10 is example burning voltage data for the empty reactor, i.e. operating as a DBD.

Fig. 10 shows that as applied voltage decreases, that burning voltage increases. The burning voltage is seen to plateau with increasing applied voltage, from ~7 kV up to 10 kV where it has a value of 2.07 kV +/− 0.1. This result contrasts that of Peeters and van de Sanden [14], who found the opposite trend to be true, i.e. burning voltage increases with applied voltage. This difference in result is likely to be due to differences in reactor geometry, as well as an increase in the reactor temperature reducing the gas breakdown strength.

Using a 300–500 μm $BaTiO_3$ packing material as an example the change in burning voltage measured as a function of applied voltage to the reactor is presented in Fig. 11.

In contrast to the DBD example in Fig. 10. Fig. 11 shows that with increasing applied voltage the burning voltage in the PBR

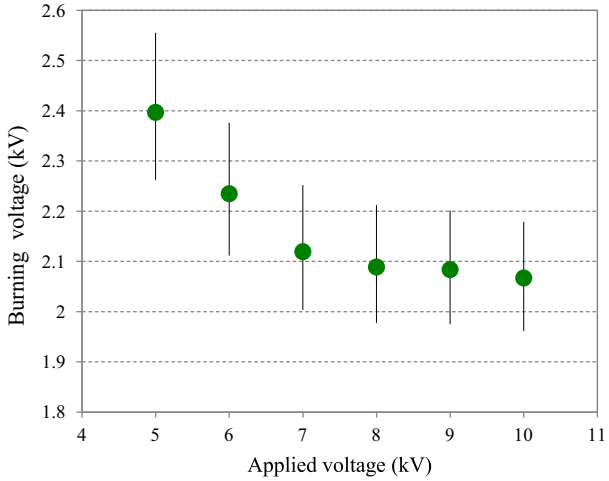

Fig. 10. Burning voltage of the empty reactor with a gas composition of 90% Ar–10% CO_2 at a total flowrate of 100 ml/min. Reactor is driven by a 5 kHz sine wave with voltages ranging between 5 and 10 kV.

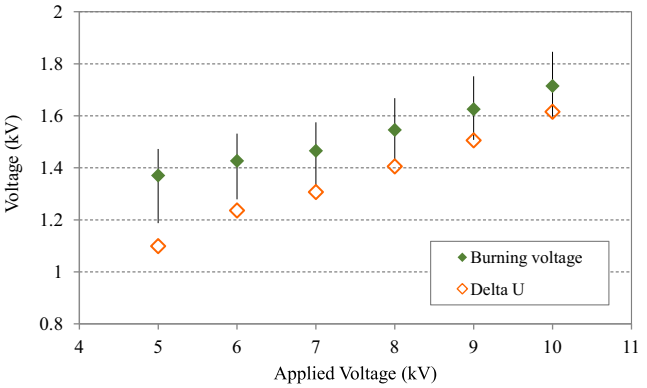

Fig. 11. Burning voltage and ΔU measured as a function of applied voltage for 300–500 μm $BaTiO_3$ particles in 90 Ar–10% CO_2 driven by a 5 kHz sine wave.

increases. This may be due to higher applied voltages causing local electric field strengths to exceed the threshold breakdown strength of individual void spaces in the bed. This increased breakdown strength would be due to either the size or shape of the void, or the shape of the particle on which it forms. This in turn raises the average burning voltage of the reactor, and consequently the measured burning voltage increases.

The electrical characteristics measured in this set of experiments use a sine wave for the driving potential, as opposed to the square wave that was used in the previous experiment. The use of the Lissajous figure to obtain electrical characteristics has been proven to be valid with sine waves. In order to ensure that the observations made here can be applied to the first set of experiments, the burning voltage of a sinusoidally or square wave driven has been compared in 180–300 μm Al_2O_3 particles with a range of different gas compositions. The results indicate that, within the margin of experimental error, there is no difference between reactor burning voltages for the two wave types.

3.2.4. Relationship between burning voltage and particle size

Presented in Fig. 12 is reactor burning voltage data for the reactor operating as a PBR and a DBD under a wide range of operating conditions.

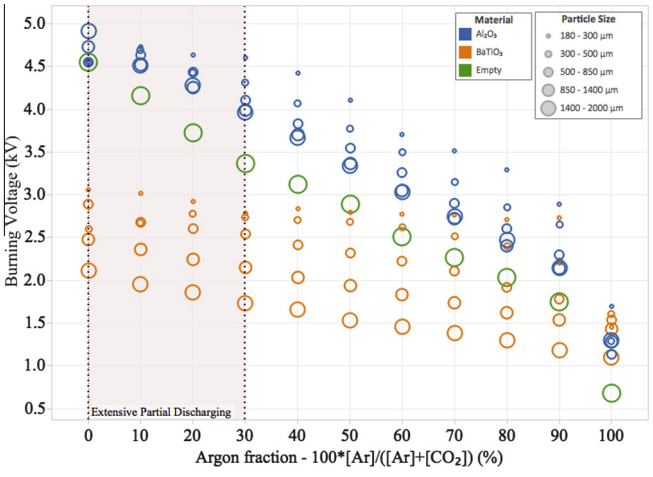

Fig. 12. Reactor burning voltage as a function of feed gas argon concentration balanced with CO_2. Applied voltage is 10 kV, with a sine wave at 5 kHz. The "extensive partial discharging" region indicates an area where the data obtained becomes less reliable due to the signal-to-noise ratio of the Lissajous figure decreasing.

The first trend to identify from Fig. 12 is the almost linear increase in reactor burning voltage with decreasing argon concentration that is observed with every reactor packing condition. The only exception to this linearity is the difference between 100% Ar, and 90% Ar–10% CO_2. This can be explained by the dramatic differences in electron transport properties between Ar and CO_2, i.e. the electron mean free path in CO_2 being much shorter than Ar, and the presence of excited states that are excited by low electron energy electrons in CO_2. T

Fig. 12 shows that, as predicted, burning voltage strongly increases with decreasing particle size. The trend is strongest with the $BaTiO_3$ packed reactor. Take, for example 1400–2000 μm $BaTiO_3$ particles, at 60% Ar–40% CO_2- feed gas composition, the burning voltage is 1.45 (±0.09) kV. With 180–300 μm particles, at the same gas composition, measured burning voltage is 2.78 (±0.20) kV, a 90% increase over the value obtained for the larger sized particle and an absolute increase of 1.3 kV. The difference in burning voltage between particle sizes using the Al_2O_3 packing is proportionately smaller, but is still significant. Using the same 60% Argon–40% CO_2 concentration as the example, with 1400–2000 μm Al_2O_3 particles, burning voltage is 3.02 kV (±0.18) kV, whilst with the 180–300 μm burning voltage is 3.7 (±0.24) kV. An increase of ~23%, or 0.68 kV absolute.

One of the other interesting results shown in Fig. 12 is the relative change in burning voltage compared with an empty reactor. Generally speaking, $BaTiO_3$ leads to a reduction in reactor burning voltage, where as Al_2O_3 causes an increase in burning voltage. The reduction in burning voltage shown by this data with $BaTiO_3$ reflects the experimental results for CO_2 conversion shown in Fig. 6f, where $BaTiO_3$ still leads to conversion at all applied voltages even in pure CO_2. This data also supports the findings of other research groups where dielectric packing materials are found to decrease reactor breakdown strengths [16,19,20]. The increase in burning voltage observed with Al_2O_3 is a more surprising result, as the strengthening of localised electric fields is an enhancement that has generally been attributed to all dielectric reactor packing materials, however this effect has been reported at least once in the literature previously [21]. It may be that although the onset of electrical breakdown is reduced, the burning voltage actually increases.

Fig. 13 shows the mean increase in absolute burning voltage for $BaTIO_3$ and Al_2O_3 packed beds relative to their respective 1400–2000 μm particle sizes. Both $BaTiO_3$ and Al_2O_3 show a rapid increase in burning voltage as particle size decreases.

The data shows that in a PBR the reactor burning voltage is dependent upon packing material, gas composition, particle size and applied voltage. There are likely to be other variables that effect burning voltage, namely gap size, dielectric material used on the electrodes, and the frequency of the applied voltage. As the reactor geometry is fixed, it is not possible to change the dielectric material or gap size. However, it is possible to easily measure the change in burning voltage by varying the frequency of the applied voltage. Fig. 14 shows the burning voltage for a 180–300 μm Al_2O_3 packed bed with frequencies in the range of 1–10 kHz.

Fig. 14 shows that there is a reduction in reactor burning voltage with increasing applied frequency. At frequencies of 2.5 kHz, no plasma discharge is found to occur at argon concentrations less than 20%, and at an applied frequency of 1 kHz, no breakdown occurs with argon concentrations less than 40%. Although the frequency dependence is only tested for the smallest Al_2O_3 particles, it is likely to be representative behavior for all packing materials. This suggests that frequencies in excess of 10 kHz would be beneficial for PBR experiments. Previous modeling and experimental work has demonstrated that increasing applied frequency can reduce breakdown voltage in DBDs [22].

3.2.5. Partial reactor discharging

The equivalent electrical circuit for partially discharging reactors obtained by Peeters and van de Sanden [14] is derived for usage with a conventional DBD (i.e. not packed bed) reactors. In a partially discharging DBD, not all of the residual memory charge stored on the surface of the DBD is transferred to the other electrode during a discharge cycle. As described previously, this is the case where $\zeta_{diel} < C_{diel}$ measured from the Lissajous figure. This same rule applies to packed bed reactors in that cases where the reactor is partially discharging can be determined by this reduced value for ζ_{diel}, and it can be used to quantify to what extent the reactor is partially discharging.

The Peeters [14] equivalent circuit model splits the DBD into discharging and non-discharging sections by two coefficients α and β. The coefficient α has been demonstrated to indicate the areal fraction of the DBD electrode that is not discharging. Conversely, β indicates the electrode areal fraction that is discharging. Eq. (4) is used to calculate the value of the coefficient α.

$$\alpha = \frac{C_{diel} - \zeta_{diel}}{C_{diel} - C_{cell}} \tag{4}$$

This equation can be applied to packed bed reactors, but the interpretation of the result is somewhat different. Rather than the value of alpha indicating the areal fraction of the electrode dis-

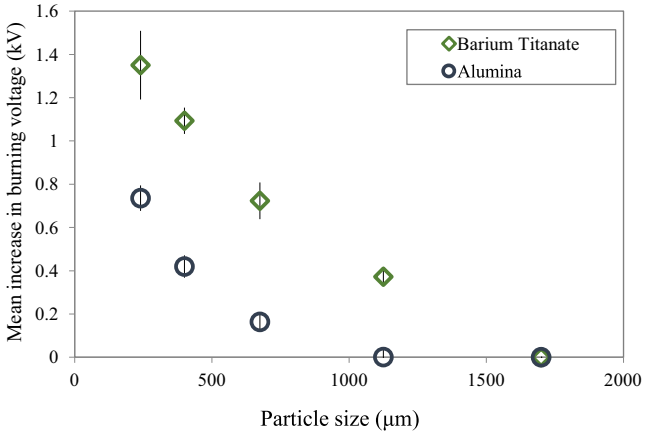

Fig. 13. Mean increase in relative reactor burning voltage taken at argon concentrations between 30% and 90% Argon for $BaTiO_3$ and Al_2O_3. Reactor is driven by a 10 kV, 5 kHz sine wave.

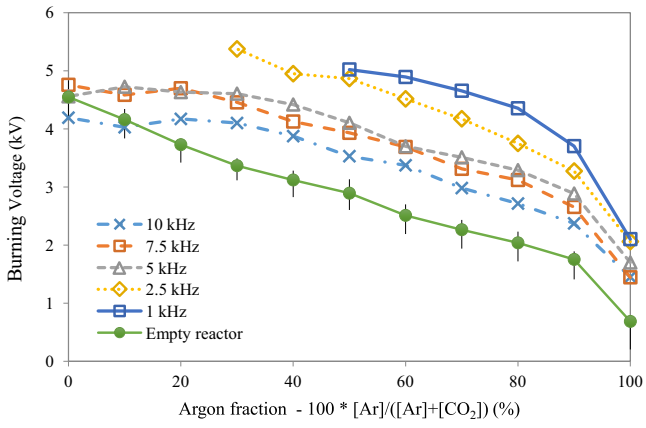

Fig. 14. Burning voltage for 180–300 μm Al_2O_3 particles as a function of frequency of the AC driving voltage, with argon–CO_2 concentrations varied from 0% to 100% operated at 10 kV. The empty reactor case is a reference and is driven by a 5 kHz sine wave. Experimental error in burning voltage measurement is no greater than 10%.

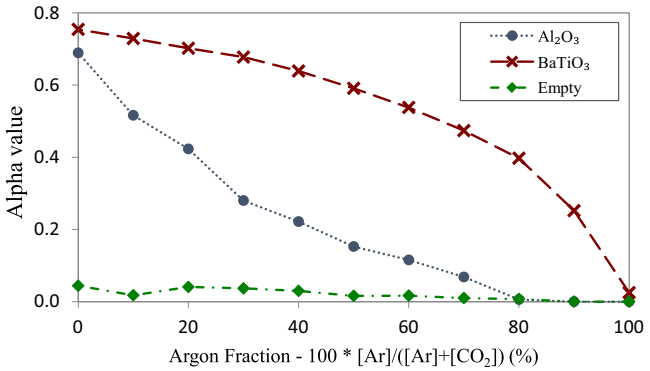

Fig. 15. α values for the packed bed reactor at different Ar–CO_2 concentrations. In cases where a packing is used the reactor packing particle size is 180–300 μm. The reactor is driven by a 5 kHz, 10 kV sine wave.

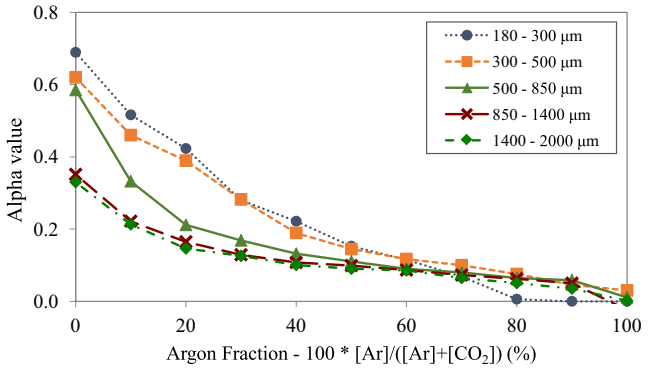

Fig. 16. α values for the alumina packed reactor with different particle sizes over a range of argon concentrations. Reactor is driven by a 5 kHz, 10 kV sine wave.

charging, it indicates the fraction of stored dielectric charge reaching the opposing electrode during a discharge cycle. With this in mind, the alpha values can be calculated for the reactor tested in this article, an example of this is shown in Fig. 15 for 180–300 μm particles and an empty reactor with varying argon and CO_2 composition.

The results shown in Fig. 15 indicate that with the unpacked reactor across all argon–CO_2 concentrations that the reactor is discharging stored charge effectively. The value of α increases to a maximum of ~0.05 in pure CO_2 with the unpacked reactor. When the reactor is packed with either $BaTiO_3$ or Al_2O_3 it can be seen that the value of alpha increases with decreasing Ar concentration. With the $BaTiO_3$, the increase in the value of α with increasing CO_2 concentration is much faster than that found with Al_2O_3 at high argon concentrations. For all argon concentrations, the value of α in 180–300 μm $BaTiO_3$ particles exceed that of Al_2O_3. This effectively means that proportionately less stored dielectric charge is "bridged" between the electrodes in the $BaTiO_3$ packed reactor, than in the Al_2O_3 reactor and the empty reactors. This may be due to the higher local charge storage capacity of $BaTiO_3$ compared with Al_2O_3 effectively trapping larger charges on its surface. The reduced burning voltage of $BaTiO_3$, indicating that localised electric field gradients are higher than for the Al_2O_3 case, also supports this hypothesis.

It should be noted however that the gas breakdown properties are also highly dependent upon reactor temperature, as well as the previous condition that the reactor was being operated in. The value of α for 180–300 μm Al_2O_3 in this experiment is approximately 0.69 with 100% CO_2 feed gas. In the previous experiment, where CO_2 conversion was measured, it was not possible to ignite a plasma in the bed with a pure CO_2 feed gas, i.e. if measured value of α would have been equal to 1. This ability to operate the reactor in pure CO_2 in this experiment may be due to residual heat from previous experiments allowing the gas to be ionised more easily [23], residual charge or metastable plasma species from prior experiments reducing the burning voltage [24].

Importantly, the value of alpha is found to have a strong particle size dependence (Fig. 16). The data shows that partial discharging occurs more readily in small particle sizes, particularly when the argon concentration is less than 50%. Given that smaller particle sizes lead to a higher burning voltage, this lower threshold and greater tendency for partial discharging is an expected, but important, result.

3.3. Evidence for change in plasma behavior with particle size and packing material

There is strong evidence that small particle sizes, insufficient applied voltages, or high CO_2 concentrations lead to partial reactor discharging. However, partial discharging is not the only change in reactor behavior that is induced by reducing the particle size. Small particle sizes are also observed to lead to very large increases in conversion in some cases.

The highest CO_2 conversion is achieved with the use of 180–300 μm Al_2O_3 particles. There are 3 possible reasons for this enhancement to conversion; a catalytic effect induced by the Al_2O_3, an enhancement of the plasma discharge within the packed bed that happens to promote CO_2 reduction, or a combination of both effects. It is not within the scope of this article to determine whether or not Al_2O_3 is catalytic in plasma for CO_2 reduction. Although there is evidence that shows that plasma can induce a paramagnetic state in Al_2O_3, which may give it some catalytic properties [9].

Voltage and instantaneous current data shows that the nature of the plasma discharge within the bed changes significantly with particle size, gas composition and packing material. Fig. 17 shows representative examples of the applied voltage and resultant instantaneous current in various reactor set-ups in a 90% Ar–10% CO_2 gas mix, all using an applied voltage of 10 kV. The most apparent feature of this figure is the magnitude of the current pulses in the 180–300 μm Al_2O_3 packed bed. Compared with every other reactor set-up, there is a large number of very high magnitude, short duration pulses. These pulses appear to be a noisy signal in the Al_2O_3 Lissajous figures – this is the result of high energy current pulses causing a step change in the charge transfer measured by the monitor capacitor. It is possible that these large magnitude, high energy pulses, combined with good gas-plasma contacting in the tightly packed bed, cause the very high CO_2 conversion observed under these reaction conditions. On the contrary, the magnitude and number of current pulses in the 180–300 μm $BaTiO_3$ packed bed is lower than in all of the other conditions tested, yet at 10 kV (and per watt of plasma power at high powers) the CO_2 conversion exceeds that in the empty reactor and all of the other $BaTiO_3$ packed beds. The exact cause of the increased CO_2 conversion under certain conditions is not clear, and requires further investigation. Changes to the nature of plasma discharges in confined spaces has previously been documented [25,26], but it is difficult to quantify the effect it has on the chemistry of the plasma. Brehmer et al. [27] have demonstrated that at a constant pressure, CO_2 reduction to CO in a DBD is related by a scaling parameter to the total transferred charge during the residence time of the gas – this can be considered as an adaptation of residence time for plasma reactors. The scaling parameters used by Brehmer et al. could be applied to PBRs to assist in isolating the effect of changes in plasma discharge behaviour.

The changes to plasma discharge phenomena can also be observed through Lissajous figures. Comparison between single shot Lissajous plots (Fig. 18) for the various reactor set-ups reveals

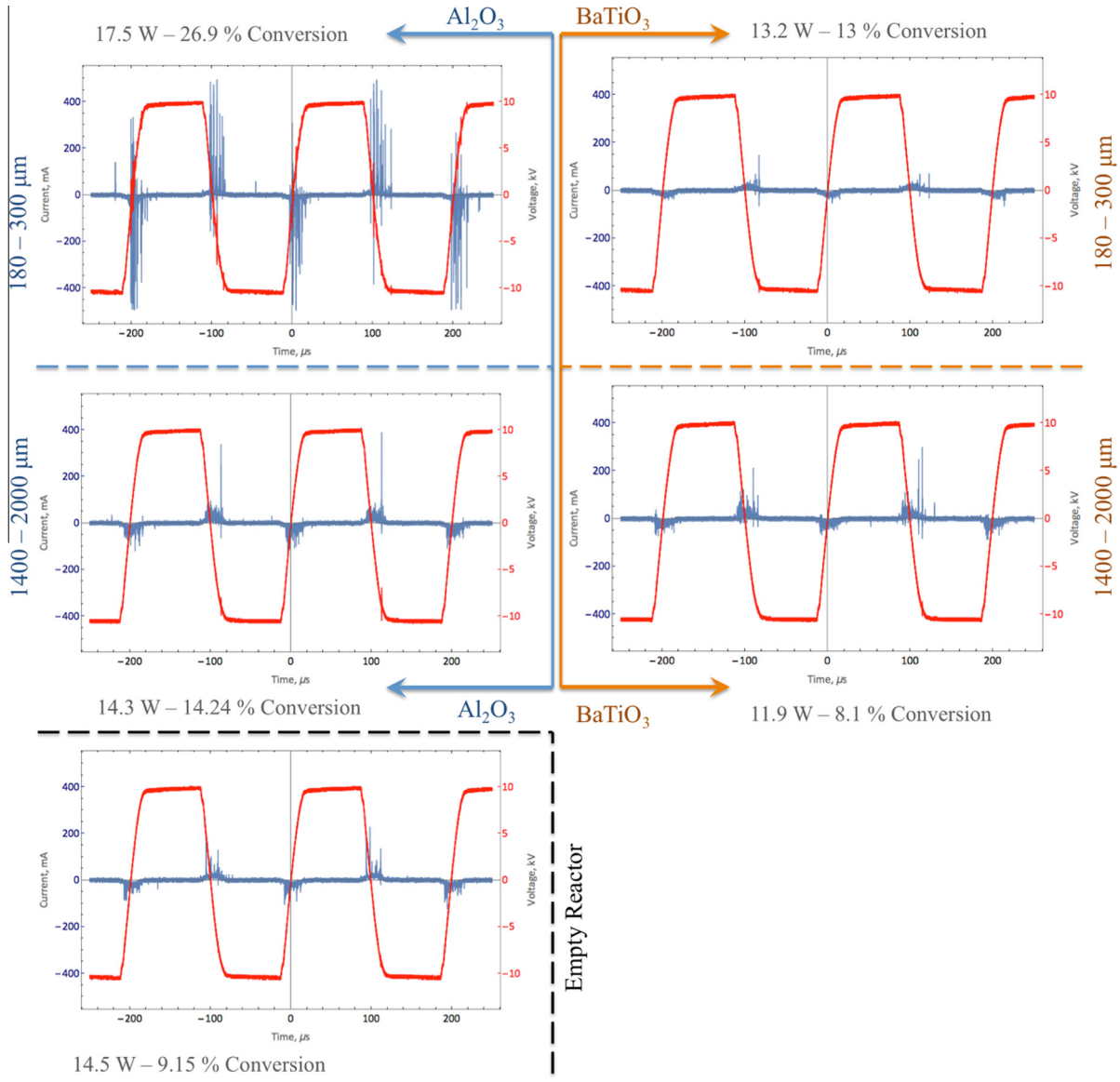

Fig. 17. Voltage and instantaneous current signals in an Al_2O_3 packed, $BaTiO_3$ packed, and empty reactors operated in 90% Ar–10% CO_2. Driving voltage is a 10 kV, 5 kHz squarewave. These samples are representative of the typical signals obtained from the oscilloscope with the stated operating conditions.

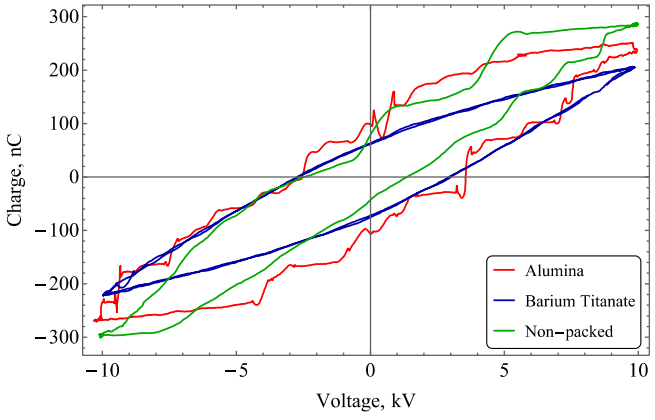

Fig. 18. Single shot Lissajous figures for 180–300 µm alumina, 180–300 µm barium titanate and a non-packed reactor, driven by a 10 kV, 5 kHz sine wave in 90% Ar–10% CO_2. A Savitzky–Golay filter is applied to smooth the data.

clear differences in discharge phenomena. Taking a single shot Lissajous figure reveals individual discharges within the PBR that do not recur identically during subsequent cycles, as is shown by the Al_2O_3 packed and non-packed reactors in Fig. 18. Clearly there are also large differences in the shape of Lissajous figures, indicating that the mechanism of charge transfer in the reactor is also different in each case. Although these plots show a change in the behaviour of the discharge, the mechanism of the discharge within the bed is not currently known. It is essential for the future development of PBRs that this behavior is understood.

4. Discussion

This work shows that small particle sizes can be beneficial for reduction of CO_2 in PBRs. However, the conditions tested suggest that the usage of noble gasses is essential in order to reap the benefits of small particle sizes. This is due to an increase in the reactor burning voltage and tendency towards partial discharging with decreasing particle sizes. The addition of argon to CO_2 can reduce the burning voltage of the mixture, and allow discharges to form

in packed bed void spaces at lower voltages than they would typically occur in pure CO_2. However, the maximum electric field strengths used in the article are relatively low (~1.7 kV/mm). This raises an important question, is it possible to gain the benefits of small particle sizes without the addition of noble gasses if stronger electric fields are applied?

In short, yes – it is possible. Duan et al. [28] have demonstrated this using a packed bed DBD microplasma reactor for conversion of CO_2 from pure CO_2 streams. By applying 9 kV to a 6 mm discharge gap, the electric fields strengths tested are approximately 10 times stronger than those in this article. Maximum CO_2 conversion is found to be much higher in 180–250 μm MgO particles (max conv. 32.8%) compared with 250–420 μm particles (max conv. = 22.6%).

The experimental work in this article and in the study by Duan et al. are two opposing cases that lie at either end of the range of electric field strengths that are being tested in PBRs. Further comparison with the work of other researchers shows that quite often, insufficient electric field strengths are applied in PBRs for complete reactor discharging to occur. Packing materials for plasma catalysis should be tested with equivalent reactor operating conditions. It is therefore important to ensure that either: (a) the reactor is fully discharging, or (b) partial reactor discharging is quantified.

In order to illustrate the importance of this, the work of some other authors is considered. To date, reporting of effective dielectric capacitance in PBRs is an uncommon practice. Mei et al. [16], Tu et al. [19] and Dou et al. [2] are the only authors to publish values for effective dielectric capacitance in their work. Mei et al. [16] and Tu et al. [19] show reduced values for ζ_{diel} compared with C_{diel} under all reactor operating conditions, and both state that this indicates that the reactor is partially discharging.

In the study by Mei et al., 2 packing materials, $BaTiO_3$ and glass, are used and compared with an empty reactor having a discharge gap of 3 mm. The effective dielectric capacitances are reported at equal powers, but different applied voltages. They find that the presence of $BaTiO_3$ in the discharge gap assists charge transfer between the electrodes compared with the empty reactor. For $BaTiO_3$ at 50 W applied power (V = 7.65 kV) the value of α = 0.12. For the same applied power using the glass packed (V = 8.45 kV), and the empty reactor (V = 7.05 kV) the values of α are 0.45 and 0.48 respectively. The authors state that for both $BaTiO_3$ and glass beads, charge transfer between electrodes is enhanced by the presence of the packing materials. This is true of the $BaTiO_3$ case, as the alpha value is very low compared with the empty reactor, and the difference in applied voltage is only 0.6 kV. However, if the glass packed reactor and the empty reactor were compared at equal applied voltages, for example 8 kV, the value for α in the glass packed reactor would be higher than in the empty reactor. This actually suggests that the glass packed reactor is blocking charge transfer between the electrodes for the same applied voltage.

Tu et al. [19] demonstrate that the use of a reduced NiO/Al_2O_3 packing material leads to improved charge transfer compared with an empty reactor. Although the data is not included, the authors state that using a non-reduced NiO catalyst, or Al_2O_3 packing alone reduces the transferred charge in the plasma compared with the reduced Ni catalyst. This suggests that non-conductive catalysts can inhibit charge transfer, leading to partial discharging. Dou et al. [2] use ceramic Raschig rings as a packing in a DBD, and observe that the measured effective dielectric capacitance when using the rings is always less than in the non packed reactor, even at the highest applied voltages. This provides further evidence that packing materials can inhibit charge transfer.

Previous studies on the effects of particle size [2,3,5,28–30] in PBRs have not reached an overall consensus on the optimum particle size. This is due to an inherent variability in the conditions that are used – reactor geometry, packing material properties and process gas all have an effect. Prior to this study, it has been identified that smaller particle sizes may inhibit formation of a discharge in the void spaces of the packed bed [30]. In addition to this, other negative effects that are likely to occur with decreasing particle size are a reduction in reactor residence time [5], an increase in pressure drop through the bed, as well as an increased loss rate of reactive species and electrons. On the other hand, there are also many potential positive effects from decreasing particle size:

- An increase in the number density of contact points [28], where discharges tend to initiate due to magnification of the electric field [5].
- Increase the density of "sharp edges" on which filamentary discharges can occur [3,4].
- Increased solid-plasma surface area for heterogeneous catalytic reactions.
- In fully discharging reactors, with small particle sizes the volume fraction of the bed occupied by plasma should be greater, i.e. improved gas-plasma contacting.

Other effects that occur with a reduction in particle size are changes to localized electric field strengths, and most importantly, a change in the nature of the discharge [29]. For example, surface discharges [4] (or some other, as yet, unidentified discharge mechanism) may become increasingly dominant over microdischarges in packed beds with small particle sizes.

However, with consideration of all of the possible effects listed, this work demonstrates that if insufficient electric field strength is applied in a PBR, that the dominant effect with reducing particle size is the increase in reactor partial discharging caused by the inability to ignite a discharge in the void spaces of the packing material. This is due to increasingly small particle sizes leading to an increase in the burning voltage of the reactor. The magnitude of the change in burning voltage is dependent on a number of parameters and is therefore variable; consequently each case should be individually assessed. In many of the prior studies on particle size in PBRs, it is possible to explain the trends observed through the occurrence of partial discharging.

Questions remain regarding the nature of plasma in a fully discharging reactor; does the change in the plasma discharge properties cause the observed increase in CO_2 conversion, or is it caused by enhanced surface chemistry of the packing material?

5. Conclusions

The efficacy of CO_2 reduction in PBRs is strongly affected by particle size, and therefore it is an important parameter. Small particle sizes (180–300 μm) increase CO_2 conversion in PBRs by up to 70%. However, small particle sizes also increase reactor breakdown voltage and the incidence of reactor partial discharging. Partial discharging is a decrease in the fraction of the reactor where plasma formation occurs. It is caused by insufficient local electric field strength, consequently reducing the overall efficacy of the reactor. Partial discharging can be avoided by applying electric fields greatly in excess of the reactor burning voltage.

For a fair comparison, packing materials in PBRs should be compared when the incidence of partial discharging is found to be very low, otherwise potentially effective packing materials may be inadvertently neglected. Reactor burning voltage and the occurrence of partial discharging can be quantified through the use of Lissajous figures with the partial discharging equivalent electrical circuit derived by Peeters and van de Sanden [14]. Partial discharging in PBRs is found to be a surprisingly common phenomenon in published literature. As such the recommendation of this article is that for PBR experiments, partial discharging should always be quantified.

Acknowledgments

A thank you is owed to Dr. Floran Peeters from DIFFER for many useful discussions via email and at the International Symposium on Plasma Chemistry. The authors gratefully acknowledge funding for this work from The University of Sheffield and EPSRC under the 4CU Programme Grant (EP/K001329/1).

References

[1] J.C. Whitehead, Plasma catalysis: a solution for environmental problems, Pure Appl. Chem. (2010) 1329.
[2] B. Dou, F. Bin, C. Wang, Q. Jia, J. Li, Discharge characteristics and abatement of volatile organic compounds using plasma reactor packed with ceramic Raschig rings, J. Electrostat. 71 (5) (2013) 939–944. 10.
[3] K. Takaki, S. Takahashi, S. Mukaigawa, T. Fujiwara, K. Sugawara, T. Sugawara, Influence of pellet shape of ferro-electric packed-bed plasma reactor on ozone generation and NO removal, Int. J. Plasma Environ. Sci. Technol. 3 (1) (2009).
[4] H.J. Gallon, X. Tu, J.C. Whitehead, Effects of reactor packing materials on H_2 production by CO_2 reforming of CH_4 in a dielectric barrier discharge, Plasma Processes Polym. 9 (1) (2012) 90–97.
[5] K.V. Laer, A. Bogaerts, <https://www.researchgate.net/publication/281174406_Improving_the_Conversion_and_Energy_Efficiency_of_Carbon_Dioxide_Splitting_in_a_Zirconia-Packed_Dielectric_Barrier_Discharge_Reactor>.
[6] E.C. Neyts, A. Bogaerts, Understanding plasma catalysis through modelling and simulation—a review, J. Phys. D Appl. Phys. 47 (22) (2014) 224010.
[7] H.-H. Kim, Y. Teramoto, N. Negishi, A. Ogata, A multidisciplinary approach to understand the interactions of nonthermal plasma and catalyst: a review, Catal. Today 256 (1) (2015) 13–22. 2015 11/1.
[8] L.B.F. Juurlink, P.R. McCabe, R.R. Smith, C.L. DiCologero, A.L. Utz, Eigenstate-resolved studies of gas-surface reactivity: CH_4 (ν 3) dissociation on Ni (100), Phys. Rev. Lett. 83 (4) (1999) 868.
[9] U. Roland, F. Holzer, A. Pöppl, F.D. Kopinke, Combination of non-thermal plasma and heterogeneous catalysis for oxidation of volatile organic compounds: part 3. Electron paramagnetic resonance (EPR) studies of plasma-treated porous alumina, Appl. Catal. B Environ. 58 (3–4) (2005) 227–234. 6/28/.
[10] A. Fridman, Plasma Chemistry, Cambridge University Press, 2008.
[11] D.E. Ashpis, M.C. Laun, E.L. Griebeler, Progress Toward Accurate Measurements of Power Consumptions of DBD Plasma Actuators. http://www.sti.nasa.gov: Center NGR; 2012 NASA/TM–2012-217449.
[12] T.C. Manley, The electric characteristics of the ozonator discharge, Trans. Electrochem. Soc. 84 (1943) 83–96.
[13] U. Kogelschatz, Dielectric-barrier discharges: their history, discharge physics, and industrial applications, Plasma Chem. Plasma Process. 23 (1) (2003) 1–46. 2003/03/01. English.
[14] F.J.J. Peeters, MCMvd. Sanden, The influence of partial surface discharging on the electrical characterization of DBDs, Plasma Sources Sci. Technol. 24 (1) (2015) 015016.
[15] P. Reichen, A. Sonnenfeld, R. Ph Rudolf von, Discharge expansion in barrier discharge arrangements at low applied voltages, Plasma Sources Sci. Technol. 20 (5) (2011) 055015.
[16] M. Danhua, Z. Xinbo, H. Ya-Ling, D.Y. Joseph, T. Xin, Plasma-assisted conversion of CO_2 in a dielectric barrier discharge reactor: understanding the effect of packing materials, Plasma Sources Sci. Technol. 24 (1) (2015) 015011.
[17] M. Ramakers, I. Michielsen, R. Aerts, V. Meynen, A. Bogaerts, Effect of argon or helium on the CO2 conversion in a dielectric barrier discharge, Plasma Process. Polym. (2015).
[18] V Goujard, J-M Tatibouët, C. Batiot-Dupeyrat, Carbon Dioxide Reforming of Methane Using a Dielectric Barrier Discharge Reactor: effect of Helium Dilution and Kinetic Model, Plasma Chem. Plasma Process. 31 (2) (2011) 315–325 (English).
[19] T. Xin, J.G. Helen, V.T. Martyn, A.G. Peter, J.C. Whitehead, Dry reforming of methane over a Ni/Al_2O_3 catalyst in a coaxial dielectric barrier discharge reactor, J. Phys. D: Appl. Phys. 44 (27) (2011) 274007.
[20] X. Tu, B. Verheyde, S. Corthals, S. Paulussen, B.F. Sels, Effect of packing solid material on characteristics of helium dielectric barrier discharge at atmospheric pressure, Phys. Plasmas 18 (8) (2011) 080702.
[21] K. Schmidt-Szalowski, S. Jodzis, K. Krawczyk, M. Mlotek, A. Gorska, Non-equilibrium plasma processes in heterogeneous systems at atmospheric pressure, Current Top. Catal. 5 (2006) 39–68.
[22] R. Valdivia-Barrientos, J. Pacheco-Sotelo, M. Pacheco-Pacheco, J.S. Benítez-Read, R. López-Callejas, Analysis and electrical modelling of a cylindrical DBD configuration at different operating frequencies, Plasma Sources Science Technol. 15 (2) (2006) 237.
[23] A. Gutsol, A. Rabinovich, A. Fridman, Combustion-assisted plasma in fuel conversion, J. Phys. D: Appl. Phys. 44 (27) (2011) 274001.
[24] R. Brandenburg, Z. Navrátil, J. Jánský, P. St'ahel, D. Trunec, H.E. Wagner, The transition between different modes of barrier discharges at atmospheric pressure, J. Phys. D: Appl. Phys. 42 (8) (2009) 085208.
[25] K. Hensel, S. Katsura, A. Mizuno, DC microdischarges inside porous ceramics, Plasma Sci. IEEE Trans. 33 (2) (2005) 574–575.
[26] K. Hensel, Microdischarges in ceramic foams and honeycombs, Eur. Phys. J. D 54 (2) (2009) 141–148. English.
[27] F. Brehmer, S. Welzel, M.C. Mvd Sanden, R. Engeln, CO and byproduct formation during CO_2 reduction in dielectric barrier discharges, J. Appl. Phys. 116 (12) (2014) 123303.
[28] X. Duan, Z. Hu, Y. Li, B. Wang, Effect of dielectric packing materials on the decomposition of carbon dioxide using DBD microplasma reactor, AIChE J. 61 (3) (2015) 898–903.
[29] M.-G. Chen, A. Mihalcioiu, K. Takashima, A. Mizuno, Catalyst size impact on non-thermal plasma catalyst assisted deNOx reactors, in: K. Yan (Ed.), Electrostatic Precipitation, Springer, Berlin Heidelberg, 2009, pp. 681–684.
[30] A.M. Montoro-Damas, J.J. Brey, M.A. Rodríguez, A.R. González-Elipe, J. Cotrino, Plasma reforming of methane in a tunable ferroelectric packed-bed dielectric barrier discharge reactor, J. Power Sources 296 (2015) 268–275.